

Flow Pattern Investigation of Savonius Cross-flow Hydrokinetic Turbine Using CFD URANS Turbulence Models

Ali Heydari ¹, Amirmasoud Mohammadi ², Amirhossein Mohammadi ³, Altug Tosun ^{*4}

¹ Department of New Energy, China University of Petroleum – Beijing,

Changping District, Fuxue Road, Beijing, China; ali.heydari@student.cup.edu.cn

² Department of Mechanical and Civil Engineering, Technical University of Denmark (DTU), Copenhagen, Denmark; S220068@dtu.dk

³ Technical Science Department of Civil and Architectural Engineering, Aarhus University, Aarhus, Denmark; 202202957@post.au.dk

^{*4} Department of Applied Mathematics and Computer Science, Technical University of Denmark (DTU), Copenhagen, Denmark; altto@dtu.dk

Abstract - The utilization of hydrokinetic turbine technology represents an innovative and sustainable approach for generating electricity by harnessing the power of flowing water. Unlike traditional hydropower plants, hydrokinetic turbines offer several advantages as they do not require the construction of dams or large water reservoirs. This characteristic eliminates potential risks to local ecosystems and communities. By directly installing these turbines in waterways, the utilization of natural resources becomes more efficient and environmentally friendly. Consequently, this technology has the potential to provide clean and reliable electricity globally while also mitigating greenhouse gas emissions and addressing climate change. This research project focuses on conducting a comprehensive investigation through two-dimensional computational fluid dynamics simulations of a cross-flow hydrokinetic turbine model. By utilizing various Unsteady Reynolds-Averaged-Navier-Stokes models, the obtained results will be compared with previous experimental and CFD models. The flow field patterns will be analysed and compared to effectively illustrate the discrepancies and similarities among different turbulence models used.

Keywords: Savonius Hydrokinetic Turbine; Renewable Energy Harvest; Flow Field Investigation; CFD simulation; URANS models; Computational Techniques;

1. Introduction

Renewable energy sources have been playing an increasingly significant role in global energy production in recent years, contributing around 2179 GW or approximately 34% of global installed power capacity. Hydropower is the most prominent contributor, accounting for around 1,151 GW or roughly 18% of the total capacity [1]. However, given the current climate crisis and the ever-growing global demand for electricity, it is critical to accelerate this trend and shift toward a renewable energy-dominated portfolio that significantly reduces carbon emissions within the next ten years[2]. This can be achieved by rapidly expanding the deployment of cost-effective and mature renewable energy conversion technologies such as solar, hydro, and wind turbines for utility-scale projects and markets[3]. In addition, efforts should be focused on developing new renewable energy industries and markets that can extract untapped renewable energy reserves, such as low-head hydropower and hydrokinetic power from water currents and waves, using next-generation energy conversion technologies. Studies on the opportunities for energy development in water conduits, for example, provide valuable insights into available opportunities and pave the way for accelerated development [4]. Fig. 1 illustrates a type of energy conversion system [5].

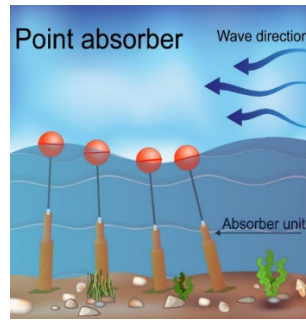


Fig. 1. A type of hydrokinetic energy conversion system. [5]

Innovative technologies have been developed in recent years, including low-head hydro technologies that can efficiently generate electricity at low heads of approximately 3 meters (9 feet) and near-zero head hydrokinetic (HK) devices, also known as current energy conversion (CEC) technologies, that can generate power without requiring local potential energy heads. According to the European Small Hydropower Association (ESHA) [6], low-head hydropower refers to electricity generation devices that can sustainably convey water at relatively low-pressure heads (up to 30 meters). HK energy, on the other hand, falls under the "zero-head" category. The conditions that create opportunities for low- to zero-head installations typically arise in various hydraulic structures such as irrigation canals, rivers, low-height dams, gauging weirs, and outflow structures. HK turbines can also be installed in canal sections where there is sufficient flow volume, velocity, and flow reliability [7]. These HK opportunities enable the exploration of new application areas and may unlock new potential in previously unexplored territories, such as flat and long river/canal sections where conventional hydropower, in the form of available potential energy, does not exist.

Simplicity, self-starting capability and omnidirectional performance are some of the excellent characteristics of Savonius type hydrokinetic turbines that attract the researchers. Various efforts have been done to predict and optimize Savonius cross-flow hydrokinetic turbines performance and to investigate flow-field patterns. Dewan et al. [8] provided a comprehensive review on previous literature as well as comparison of different RANS models performance in simulation and performance prediction of Savonius turbines. They claimed that SST $k-\omega$ is the most accurate RANS model for simulation of Savonius turbines; however, they also indicated the lack of high-fidelity research simulations such as LES model within this subject. Sharma and Sharma [9] used $k-\epsilon$ and SST turbulence models for simulation of a Savonius rotor with multiple miniature blades layered on a water Savonius rotor. They concluded that SST model seems to be more accurate for their 3-D numerical simulation. Kumar et al. [10] also validated their 3D computational analysis of hydrokinetic Savonius turbine using RSM, SST transition, Realizable and Standard $k-\epsilon$ models with wind tunnel experimental results of Hayashi et al. [11]. The results illustrated that Realizable $k-\epsilon$ has the most reliable agreement with prior experimental data. Talukdar et al. [12] made a 2-D computational and experimental analysis of two and three-bladed Savonius water turbine which showed the supremacy of two-bladed type. They further compared semi-circular and elliptical profiles for the two-bladed rotor. They concluded that elliptical blade would result in the turbine inferior performance.

Computational Fluid Dynamics (CFD) investigations have become an essential tool in the development and simulation of hydrokinetic turbines. By utilizing CFD we can investigate the complex flow fields and fluid-structure interactions that occur in hydrokinetic turbines, allowing for more accurate predictions of the turbine's performance and efficiency. Choosing a specific URANS model depends on factors such as flow characteristics, available computational resources, and desired level of accuracy. Each model has its strengths and weaknesses in capturing different aspects of turbulent flows. Conducting sensitivity analyses or validation studies can help determine the most suitable model for simulating a hydrokinetic turbine under specific operating conditions. The purpose of present study is to simulate a vertical axis cross-flow hydrokinetic turbine using different turbulence models, and compare and validate the modelling with performance parameters of previous literature experimental results; then output flow patterns are brought and discussed in details to justify the accuracy of models and compare the output resolutions.

2. Numerical Methodology

In this study, the Navier-Stokes equations have been solved with the commercial CFD software ANSYS FLUENT 2022 R2. The code is based on solving governing equations with a finite volume discretization technique. This method is a very popular and easier to implement for unstructured meshes.

No single turbulence model is universally accepted as being superior for all classes of problems. The choice of turbulence model will depend on considerations such as the physics encompassed in the flow, the established practice for a specific class of problem, the level of accuracy required, the available computational resources, and the amount of time available for the simulation. [13] For the present numerical modeling, four commercially available fluent models are investigated to be compared within the present investigation: SST k- ω , Reynolds Stress-omega Model (RSM), Spalart-Allmaras (SA) and Transition SST model.

2.1. Parameter Definition

- Maximum available power:

The maximum available power contained in free-flowing water streams can be calculated based on the following equation:

$$P_{max} = \frac{1}{2} \rho AV^3 \quad (1)$$

Where P_{max} is maximum available power (W), ρ is the water density (kg/m³), A is the swept area of the turbine (m²), and V is the freestream water velocity (m/s). For a vertical-axis hydrokinetic turbine, the swept area $A = D \times H$ where D and H is the diameter and height of the turbine (m) respectively.

- Extracted mechanical power:

On the other hand, the mechanical power extracted by the turbine is given by:

$$P_{rotor} = T\omega \quad (2)$$

Where P_{rotor} is the mechanical power extracted by the turbine (W), T is the torque generated by the turbine (Nm), and ω is the angular velocity of the turbine (rad/s).

- Coefficient of power:

Since the continuity of the streaming water moving past the turbine rotor needs to be preserved, added with some losses in the process of energy conversion, only a fraction of the kinetic energy can be extracted by the turbine. This measure of turbine performance is quantified through the coefficient of power, C_p , which is the ratio between the extracted and available power, expressed as:

$$C_p = \frac{P_{rotor}}{P_{max}} \quad (3)$$

- Coefficient of torque:

In addition to the C_p , another measure of the turbine performance is the coefficient of torque (C_T), given as the ratio of the torque generated by the turbine rotor to the maximum available torque:

$$C_T = \frac{T}{\frac{1}{4} \rho D^2 H V^2} \quad (4)$$

The functional relationship between C_p and C_T , reduced from all the equations above, is:

$$C_p = C_T \times \text{TSR} \quad (5)$$

- Tip-speed ratio:

The C_p of the turbine depends on its tip-speed ratio (TSR, or λ), i.e., the ratio of the tip velocity of its rotor blades to the freestream velocity of the water, given as:

$$\text{TSR} = \frac{\omega D}{2V} \quad (6)$$

2.2. Geometry and Boundary Conditions

Fig. 2 depicts two domains which are detached by a sliding region created by means of ANSYS Design Modeler in ANSYS 2022 R2. The modeled turbine is a typical two bladed Savonius hydrokinetic turbine with semi-circular blades. The geometry of the turbine is obtained from previous experimental literature [12].

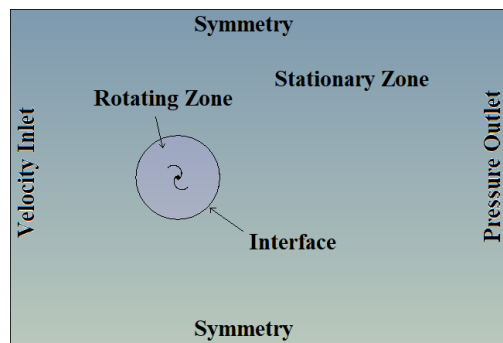


Fig. 2. Turbine geometry used for current investigation.

2.3. Meshing

In this research, the complexity of the geometry necessitated the use of a combination of quadrilateral elements for the stationary zone and triangular meshes for the rotating zone. ANSYS meshing interface was employed. To accurately represent the rotating domain, a finer mesh was utilized compared to that used for the fixed domain. Figure 3 illustrates 25 inflation layers applied to the rotor blades with a growth rate of 1.2. This specific choice aimed to capture rapid variations in velocity, pressure, and vorticity around the rotor. To ensure accuracy in computational analysis, it is important to consider non-dimensional wall distance (y^+). In this study, maintaining a y^+ value below 1 was crucial. Higher values can lead to decreased accuracy as they prevent proper determination of boundary layer behavior using ANSYS-prescribed wall functions. Furthermore, to enhance credibility and reliability, it is worth noting that an independent finding demonstrating mesh independence has been reported as part of this study.

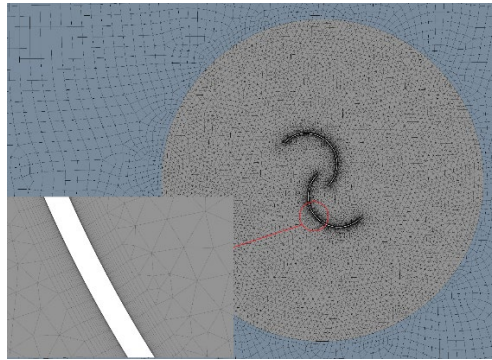


Fig. 3. The meshing used for the studied model.

3. Numerical Results

3.1. Mesh sensitivity analysis

In order to assess the impact of mesh resolution on rotor performance, a two-dimensional transient analysis was conducted. The objective was to achieve grid independence by employing three different meshes: M1, M2, and M3. These meshes consisted of approximately 90,000 nodes, 233,000 nodes, and 275,000 nodes respectively which have C_p deviation of 15%, 2% and 0% from the case with maximum number of element. Consequently, it was determined that mesh configuration M2 should be adopted moving forward due to its negligible deviation with M3 which has the highest number of mesh elements.

3.2. Validation of CFD results and Performance Characteristics

Unsteady simulations were conducted in this study to gain a deeper understanding of the water flow dynamics for turbines using different turbulence models. From Figs. 4 (a) and (b), it is observed that both C_t vs TSR and C_p vs TSR diagrams pursue similar trend for all the utilized URANS models. These values confirm the findings of contours presented in next sections that Spalart-Allmaras and RSM models predict close performance to each other which are slightly higher than the predicted performance values of SST $k-\omega$ and SST Transition models.

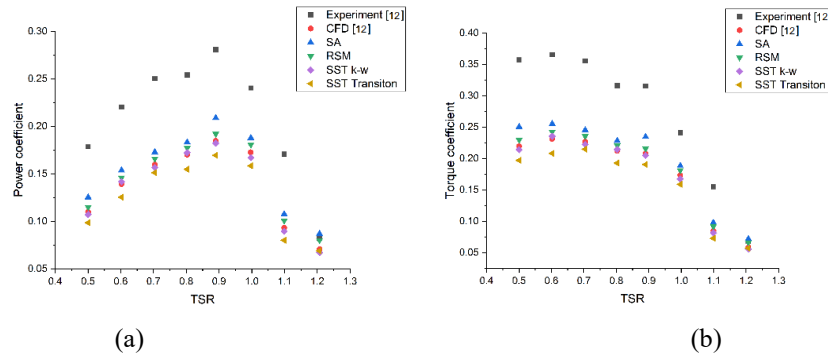


Fig. 4. Comparison of performance coefficients predicted by the utilized models (a) Coefficient of Power (b) Coefficient of Torque

3.3. Pressure

To gain insights into the time history of torque at the optimum TSR (Tip Speed Ratio) of the Savonius-type horizontal-axis turbine (SHT), pressure contours are analysed. Fig. 5 illustrates pressure contours at different azimuthal positions (θ) of the turbine when operating at a TSR value of 0.89. Upon examination, it is evident that all simulated models exhibit a relatively higher pressure zone on the concave side of the advancing blade at $\theta = 45^\circ$ and 90° compared to when positioned at $\theta = 135^\circ$. This indicates that there is a generation of higher pressure drag during these two azimuthal angles, affecting overall turbine performance. This also implies that, the amount of generated torque and therefore power, is higher at azimuthal angles equal to 45° and 90° compared to the time when turbine is at $\theta = 135^\circ$. The presence of a higher-pressure zone on the concave surface of the advancing blade and a low-pressure zone on its convex side contributes to creating a significant pressure drop,

which influences turbine rotation and power generation. Additionally, both RSM and Spalart-Allmaras models indicate greater pressure drops in their respective contours—further reinforcing their predictions for superior power extraction capabilities. These findings support previous indications that RSM and Spalart-Allmaras models yield better performance predictions due to their ability to capture more accurate drag coefficients.

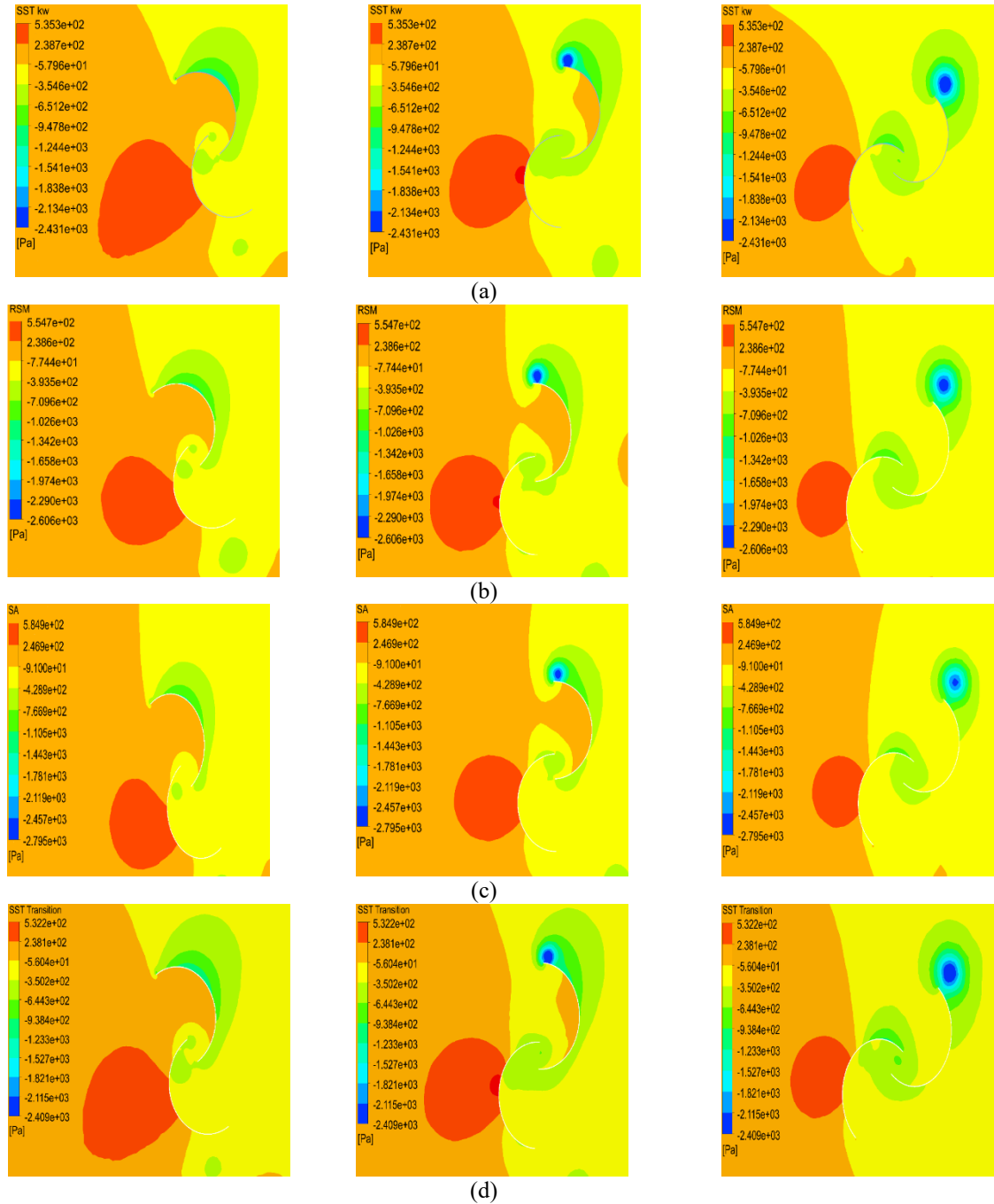


Fig. 5. Pressure contours for (a) SST $k-\omega$ model (b) RSM model (c) Spalart-Allmaras model (d) SST Transition model

3.4. Vorticity

In this section, the vorticity contours are illustrated in fig. 6. to analyse blade-wake interaction and the distribution of vorticity around the turbine blades at different azimuthal positions (θ) of 45° , 90° , and 135° for all turbulence models utilized in this study. The vorticity contours reveal similar wake structures around the turbine blades for all models employed. The SST $k-\omega$ and SST Transition models predict higher levels of turbulent wakes compared to RSM and Spalart-Allmaras models. This difference is particularly evident at the tip of the blades, overlapping regions between blades, and downstream areas. These findings suggest that SST $k-\omega$ and SST Transition models may yield lower performance predictions compared to RSM and Spalart-Allmaras models. Based on reports in previous literature [12], the higher vorticity in the mentioned areas particularly at overlapping region between the blades indicates performance degradation and implies on lower performance prediction.

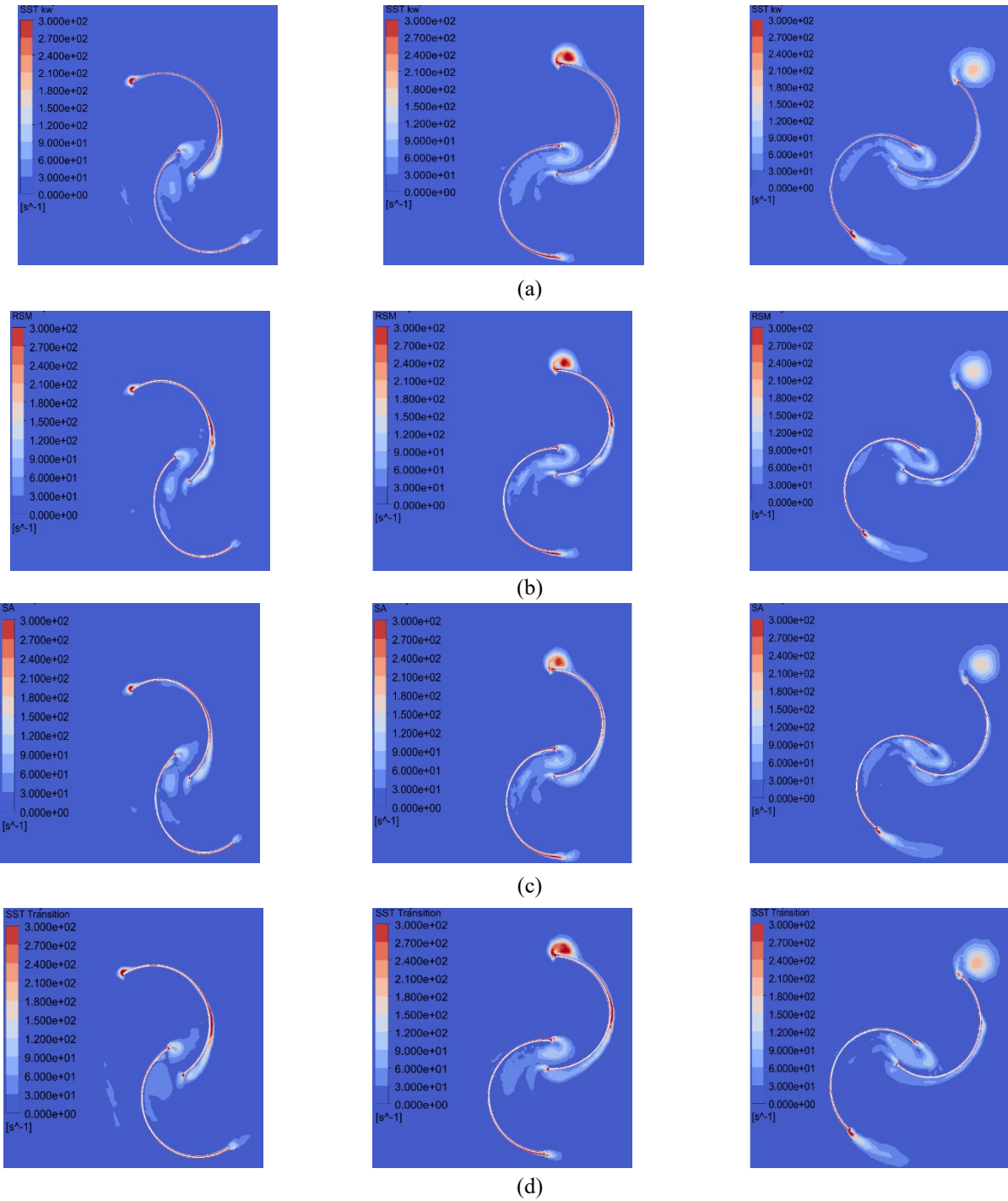


Fig. 6. Vorticity contours for (a) SST $k-\omega$ model (b) RSM model (c) Spalart-Allmaras model (d) SST Transition model

4. Conclusion

Savonius wind/hydrokinetic turbines have emerged as a promising solution for generating low-cost electricity while minimizing environmental impacts. These turbines offer decentralized energy generation, making them suitable for locations with limited or unavailable traditional power sources. To assess their efficiency and effectiveness in harnessing renewable energy, various modelling approaches have been employed. In this study, a Savonius turbine model was developed and its performance was evaluated using four different 2D URANS (Reynolds-Averaged Navier-Stokes)

models in ANSYS FLUENT software. The model was first validated against existing experimental and numerical literature. Subsequently, the SST $k-\omega$, RSM, Spalart-Allmaras, and SST Transition models were used to investigate and compare their performance prediction for hydrokinetic turbine simulation under similar operating conditions. The results indicated that the SST $k-\omega$ and SST Transition models showed similar performance and flow patterns. Conversely, the RSM and Spalart-Allmaras models, while exhibiting similarities, predicted higher performance compared to the former pair. It is worth noting that the Spalart-Allmaras model displayed unexpectedly high accuracy despite its simplicity in this particular investigation. Additionally, all models predicted similar trends for both C_p and C_t vs TSR values. Although this investigation covered the essential aspects of these effects, future research may consider 3D CFD simulations to gain a deeper understanding of the flow physics explained by these models and validate their performance predictions more comprehensively. Ultimately, utilizing both 2D and 3D approaches can lead to a more conclusive assessment of the prediction accuracy.

Acknowledgements

This work was fully supported by the National Natural Science Foundation of China (No. 52211530034)

References

- [1] M. Bilgili, H. Bilirgen, A. Ozbek, F. Ekinici, and T. Demirdelen, "The role of hydropower installations for sustainable energy development in Turkey and the world," *Renewable Energy*, vol. 126, pp. 755-764, 2018.
- [2] IPCC, "Global Warming," <https://www.ipcc.ch/>, 2018.
- [3] NREL, "Renewable Electricity Futures Study," https://www.nrel.gov/analysis/re_futures/, 2012.
- [4] M. J. Sale, N. A. Bishop Jr, S. L. Reiser, K. Johnson, A. C. Bailey, A. Frank, et al., "Opportunities for Energy Development in Water Conduits," Oak Ridge, Tennessee: Oak Ridge National Laboratory, 2014.
- [5] <https://www.energy.gov/eere/water/marine-energy-glossary>.
- [6] ESHA, "Guide on how to develop a small hydropower plant.," http://www.ee.co.za/wpcontent/uploads/legacy/01GT_Guide.pdf, 2009.
- [7] I. Loots, M. Van Dijk, B. Barta, S. Van Vuuren, and J. Bhagwan, "A review of low head hydropower technologies and applications in a South African context," *Renewable and Sustainable Energy Reviews*, vol. 50, pp. 1254-1268, 2015.
- [8] A. Dewan, S. S. Tomar, A. K. Bishnoi, and T. P. Singh, "Computational fluid dynamics and turbulence modelling in various blades of Savonius turbines for wind and hydro energy: Progress and perspectives," *Ocean Engineering*, vol. 283, p. 115168, 2023.
- [9] S. Sharma and R. K. Sharma, "CFD investigation to quantify the effect of layered multiple miniature blades on the performance of Savonius rotor," *Energy conversion and management*, vol. 144, pp. 275-285, 2017.
- [10] A. Kumar, R. Saini, G. Saini, and G. Dwivedi, "Effect of number of stages on the performance characteristics of modified Savonius hydrokinetic turbine," *Ocean Engineering*, vol. 217, p. 108090, 2020.
- [11] T. Hayashi, Y. Li, and Y. Hara, "Wind tunnel tests on a different phase three-stage Savonius rotor," *JSME International Journal Series B Fluids and Thermal Engineering*, vol. 48, pp. 9-16, 2005.
- [12] P. K. Talukdar, A. Sardar, V. Kulkarni, and U. K. Saha, "Parametric analysis of model Savonius hydrokinetic turbines through experimental and computational investigations," *Energy Conversion and Management*, vol. 158, pp. 36-49, 2018.
- [13] U. Manual, "ANSYS FLUENT 12.0," Theory Guide, 2009.